Aqueous Speciation of Tetravalent Actinides in the Presences of Chloride and Nitrate Ligands

Rameswar Bhattacharjee and Pere Miró*

Department of Chemistry, University of South Dakota, Vermillion, South Dakota 57069, United States.

Abstract

Speciation of hexachloride tetravalent uranium, neptunium, and plutonium species in aqueous media have been investigated using density functional theory in the presence of inner sphere ligands such as chloride, nitrate, and solvent molecules. All possible structures with the formula $[An^{IV}(Cl)_x(H_2O)_y(NO_3)_z]^{4-x-z}$ (An=U, Np, and Pu; x=0-6, y=0-8, and z=0-6) were considered to explore the speciation chemical space of each actinide. The nature of the mixed-ligand complexes present in solution is controlled by the concentration of free ligands in solution. A low chloride concentration is suitable to drive the speciation away from the highly thermodynamically stable hexachloride species. Furthermore, the formation of dimeric species can proceed through both olation and oxolation mechanisms. Oxolation is preferred for monomers that contain fewer water ligands, while olation becomes favorable for the complexes with more water ligands.

Introduction

Uranium, neptunium, and plutonium can all access a wide variety of oxidation states ranging from +3 up to +6, while under more extreme conditions oxidation states +2 and +7 can also be observed. Uranium ions in aqueous solution are predominately observed to be in the hexavalent state in the form of the uranyl ion;[1, 2] however, under reducing conditions U(IV) species form.[3] On the other hand, Np is most often in the +5 oxidation state in aqueous solution, while Np(IV) is stable under reducing conditions.[2, 4] Finally, plutonium can coexist as Pu(III), Pu(IV), Pu(V), and Pu(VI) in a single solution, and its redox state is strongly influenced by the experimental conditions.[2] In the absence of inner sphere ligands besides water, the reduced forms of An(IV) elements exist as hydrated cations that hydrolyze even under acidic conditions that in turn nucleate into larger aggregates through olation and oxolation reactions leading to the formation insoluble hydroxides, particularly under high concentrations. Species containing An(IV) ions are of particular interest due to their thermodynamic favorability, the insolubility of their hydrolysis products, their ability to grow into nanosized molecular metal oxides under certain conditions, and the geological relevance of actinide materials in this oxidation state.

Actinide halides ($[AnX_n]^{q-}$, X=halide) have attracted the scientific community's attention due to their use in the nuclear industry, primarily for isotope enrichment, and are among the most extensively exploited molecular units within the domain of actinide chemistry.[5-11] Furthermore, actinide halides are widely used in actinide separation processes and also have significant applications in non-aqueous transuranic chemistry.[12, 13] $[AnO_2Cl_2]^{2-}$ and $[AnCl_6]^{2-}$ are two dominating structural motifs identified for An(VI) and An(IV) chlorides, respectively.[14-16] For example, $[UO_2Cl_2]^{2-}$ and $[PuO_2Cl_2]^{2-}$ have been characterized both in solution as well as in the solid state.[17] Similarly, $[UCl_6]^{2-}$, $[NpCl_6]^{2-}$, and $[PuCl_6]^{2-}$ have been isolated and explored in the

literature.[12, 18-25] Moreover, the octahedral ligand environment in $[AnCl_6]^{2-}$ provides a suitable platform to examine the properties of actinides and compare them with transition metals in a similar coordination environment.[9, 26, 27] The presence of non-aquo inner sphere ligands limits the hydrolyzation of An(IV) species; therefore, there is a fundamental need to understand and control their speciation, especially towards the formation of intermediates capable of undergoing olation or oxolation reactions.

Herein, speciation reactions starting with $[AnCl_6]^{2-}$ (An=U, Np, and Pu) in aqueous solution in presence of nitrate were investigated using density functional theory. Understanding the role of nitrate in the speciation of actinide halide species is important since nitric acid/nitrate salts are active reagents involved in nuclear reprocessing. Specifically, all mixed ligand monomeric complexes within the set $[An(Cl)x(H_2O)_y(NO_3)_z]^{4-x-z}$ (An=U, Np, Pu and x=0-6, y=0-8 and z=0-6) were considered in order to explore the speciation chemical space of $[AnCl_6]^{2-}$ species. Different concentrations of chloride and nitrate ions were considered to explore the impact on aqueous speciation. Finally, the formation of dimeric species through olation and oxolation mechanisms from energetically accessible monomeric species with An-H_2O moieties were studied.[14]

Computational Details

All density functional theory calculations were performed using the Turbomole V7.3 suite.[28] The hybrid exchange-correlation density functional PBE0, including Grimme's D3 dispersion correction with Becke-Johnson damping D3BJ, was used for all of the geometry optimizations and frequency calculations.[29-32] The resolution of the identity (RI) approximation was used to accelerate the calculation of integrals.[33] Standard quadrature grids with the size "m4" were employed for all the calculations. The def2-TZVP basis set was used to describe all atoms with the exception of the actinides for which the def-TZVP basis set was employed.[34, 35] All stationary points were confirmed as minima by harmonic vibrational analysis. To incorporate the effect of the aqueous environment, single-point energy calculations were performed using the conductor like screening model (COSMO).[36, 37] Experimental free energy of hydration (ΔG_{hyd}) of all the free ligands and proton were used. For Cl^- and NO_3^-, the ΔG_{hyd} values were -75.8 kcal/mol and -64.5 kcal/mol, respectively.[38, 39] The hydration free energy of a single water molecule in aqueous medium was -6.3 kcal/mol,[40] while that of a proton was -265.9 kcal/mol.[41-43] All free energies are computed for 1M solutions using the usual correction term RT*ln*(24.46).[44] The concentration of water was always considered to be 55.34 M which is the bulk water concentration.

Single-point energy calculations were performed to using M06 and B3LYP-D3(BJ) with the same basis sets and solvation model as in the optimization.[45-49] In the following, the label M06 will be used for free energies computed at the M06/def-TZVP,def2-TZVP/COSMO//PBE0-D3(BJ)/def-TZVP,def2-TZVP level of theory and B3LYP will be used to refer to the B3LYP-D3(BJ)/def-TZVP,def2-TZVP/COSMO//PBE0-D3(BJ)/def-TZVP,def2-TZVP level of theory. Electronic energies, zero-point energies (ZPE), enthalpies (ΔH), and entropic ($T\Delta S$) contributions were computed at the PBE0-D3BJ/def-TZVP,def2-TZVP level of theory. All relative free energies are

computed in reference to the corresponding $[An(IV)Cl_6]^{2-}$ species. All images of the complexes are created using CYLview visualization software.[50]

Results and Discussion

The optimized geometry of $[UCl_6]^{2-}$ is in good agreement with reported experimental data. The average PBE0 U-Cl bond distance is 2.63 Å, consistent with the experimental value of 2.62 Å.[24] In aqueous solution, $[UCl_6]^{2-}$ can undergo ligand exchange reactions with nitrate and aqueous solvent molecules to form mixed-ligand complexes. The resulting mixed ligand species that are present in solution have different numbers of chloride, nitrate, and aquo ligands. The distribution of these complexes that are ultimately observed in experiment depend on their free energy of formation relative to the parent system, $[UCl_6]^{2-}$, which is thermodynamically most favorable under standard state conditions (*vida infra*). The equilibrium between different species can be controlled by systematically varying the concentration of ligands present in solution. In Figure 1, a set of ternary contour plots are presented showing the speciation of the U(IV) species as a function of ligand concentration. At standard conditions (Figure 1a), all regions in the contour diagram are endergonic showing that $[UCl_6]^{2-}$is indeed thermodynamically favored and chloride ligand exchange is not predicted to occur. On one hand, if the concentration of the nitrate ion is increased from 1 M to 10 M, there is little to no impact on the U(IV) speciation energetics (Figure 1b). On the other hand, if the concentration of chloride is reduced to 1 mM, keeping the concentration of the nitrate ion constant at 1 M, there is a substantial impact on the speciation energetics and an exergonic region is observed (Figure 1c). Therefore, at low chloride concentrations several mixed ligand species are stabilized with the most stable species predicted to be $[U(NO_3)_6]^{2-}$. All the species on the horizontal axis are U(IV) complexes with different Cl^- :NO_3^- ratios without any water ligands. This region is mostly exergonic with respect to the parent hexachloride complex. Note that only complexes with water ligands can hydrolyze into larger

aggregates. The presence of one or more water ligands has the potential to speciate further through olation or oxolation process, first forming dimeric species.

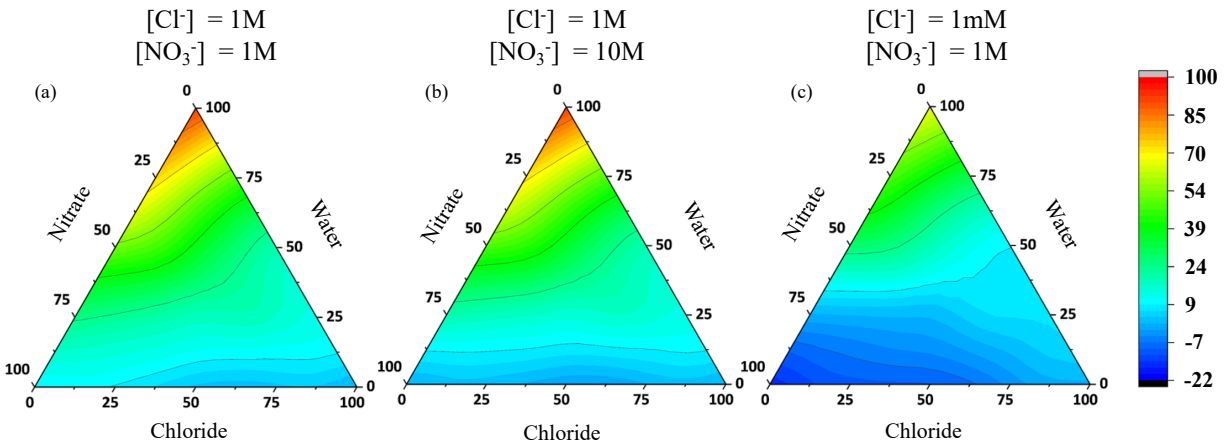

Figure 1. Ternary speciation plot for U(IV) species in aqueous media in presence of chloride and nitrate at different conditions. (a) Both chloride and nitrate are at standard state concentration of 1 M. (b) Chloride concentrations are at 1 M and the nitrate concentration is 10 M. (c) Chloride concentration is 1 mM and the nitrate concentration is 1 M. The corners of each plot correspond to the three pure complexes $[UCl_6]^{2-}$ (100% chloride, bottom right), $[U(NO_3)]^{2-}$ (100% nitrate, bottom left), and $[U(H_2O)_8]^{4+}$(100% water, top), respectively. The free energy of formation in kcal/mol of each species relative to $[UCl_6]^{2-}$ is represented by color according to the scale on the right at PBE0-D3BJ/def-TZVP,def2-TZVP/COSMO//PBE0-D3BJ/def-TZVP,def2-TZVP level of theory.

To investigate the impact of the actinide, the analogous speciation of Np(IV) and Pu(IV) were computed. The mixed-ligand complexes that are exergonic with respect to the parent hexachloride compound are similar regardless of the identity of An(IV) at a low chloride concentration (1mM) (Figure 2), although there ae small differences. Specifically, the ternary plot of Pu(IV) species has a slightly smaller exergonic region, which suggests that the chloride ligands in $[PuCl_6]^{2-}$ are less labile than in $[UCl_6]^{2-}$ and $[NpCl_6]^{2-}$. In other words, mixed-ligand Pu-complexes are less stable relative to $[PuCl_6]^{2-}$ compared to the analogous U- and Np-mixed-ligand complexes. The full profiles of the speciation of U(IV), Np(IV), and Pu(IV), containing all the possible An-mixed-ligand complexes along with their formation Gibbs free energies, are included as supporting information (Figure S6-S8).

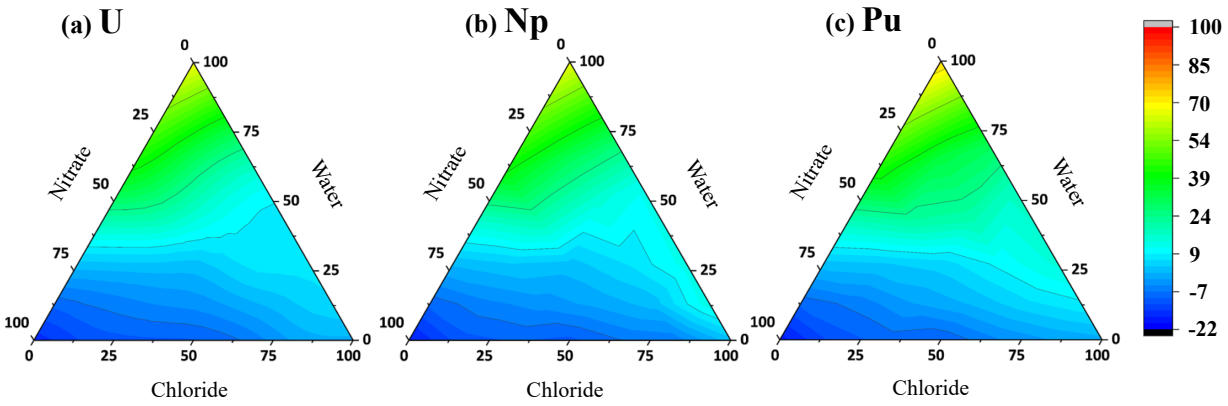

Figure 2. Ternary contour plots for the speciation of (a) U(IV), (b) Np(IV), and (c) Pu(IV), complexes in aqueous media at a chloride concentration of 1mM and nitrate concentration of 1M. The corners of each plot correspond to the three pure complexes $[AnCl_6]^{2-}$ (100% chloride, bottom right), $[An(NO_3)]^{2-}$ (100% nitrate, bottom left), and $[An(H_2O)_8]^{4+}$(100% water, top), respectively. Free energies of formation in kcal/mol of each species relative to the corresponding $[AnCl_6]^{2-}$ (An=U, Np and Pu) are represented by color according to the scale on the right at PBE0-D3BJ/def-TZVP,def2-TZVP/COSMO//PBE0-D3BJ/def-TZVP,def2-TZVP level of theory.

Several factors control the chemistry of An(IV) complexes in aqueous media but hydrolysis is one of the most important phenomena since it is responsible for the generation of An-OH species that can undergo nucleation via a series of condensation reactions to form larger clusters.[14] In aqueous solution, the An(IV) complexes with An-H_2O moieties have the propensity to undergo hydrolysis through the deprotonation of one or more aquo ligands,

$$[An(OH_2)_m]^{n+} \rightarrow [An(OH_2)_{m-h}(OH)_h]^{(n-h)+} + hH^+$$

The extent of this reaction is mainly controlled by the Brønsted acidity of the An(IV)-aquo species; however, it is also sensitive to the presence of other species in solution, concentration, temperature, and pH.[14] The hydrolyzed actinide species can then nucleate into larger aggregates through olation and oxolation reactions.[51] On one hand, in an olation reaction actinide-hydroxo moieties displace aquo ligands of another species forming hydroxo-bridged species,

$$An - OH + An_{aq} \rightarrow An - OH - An$$

On the other hand, in an oxolation reaction two actinide-hydroxo moieties condense to form a bridging oxo moiety,

$$An - OH + An - OH \rightarrow An - O - An + H_2O$$

The charge and electronegativity of An(IV) ions favor the olation products that are usually ill-defined structures and lead to amorphous precipitates unless stabilized through the presence of oxygen donor or halogen ligands.[52-62] Both mechanisms have been prosed based on experimental observation via the characterization of the respective An(IV) dimer products.[63-65] Two dimeric Pu(IV)-complexes shown in Figure 3 can be taken as an example of this. The first was reported by Hixon and co-workers where two Pu(IV) centers are connected by an oxo anion consistent with an

oxolation product (Figure 3a).[64] On the other hand, a structure that corresponds to an olation product was crystalized by Soderholm and co-workers (Figure 3b).[65] While the structures suggest that these dimers are formed by different mechanisms, computed energetics of these two mechanisms provide additional support to this hypothesis.

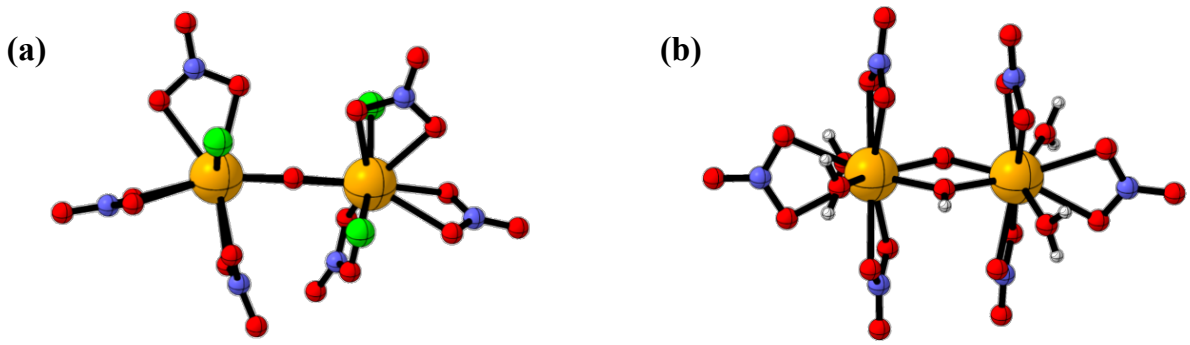

$[Pu^{IV}_2(O)(NO_3)_6(Cl)_4]^{4-}$ $[Pu^{IV}_2(OH)_2(NO_3)_6(H_2O)_4]$

Figure 3. Two Pu(IV) dimers characterized by X-ray diffraction. (a) The structure isolated by Hixon and co-workers (oloxation product) (Ref. 64), (b) The structure isolated by Soderholm and co-workers (Ref. 65) (olation product) Color scheme: Uranium in pink, chloride in green, oxygen in red, nitrogen in blue, and hydrogen in white.

First, we consider the dimerization pathways for the U(IV) species. The dimerization reactions start from the most energetically favorable U(IV) monomers. Recall that in order to generate a dimer with a bridging oxygen group, the low energy uranium-mixed ligand complexes must contain at least one water. The dimerization is first computed for monomeric species with one water. Those that meet this criterion from the complete speciation of U(IV) monomers, for low concentrations of the chloride ion, are shown in Figure 4. Analogous Np(IV)- and Pu(IV) monomeric species are provided as supporting information (Figure S8, and Figure S10). Selected bis-aqua monomers are also studied (*vida infra*). The formation Gibbs free energy of each species relative to $[UCl_6]^{2-}$ is reported. The nitrate ligand is always bidentate in the monomeric actinide species with an average bite angle of 50.0°. The stability of the monomeric complexes increases with the coordination of each additional nitrate ligand. Furthermore, the Gibbs free energy for the exchange of a chloride ligand with water decreases as the number of nitrate ligands increases (5.6 kcal/mol in $[UCl_6]^{2-}$ compared to 1.2 kcal/mol in $[UCl(NO_3)_5]^{2-}$). The effect of the exchange-correlation functional was tested by performing single point calculations using the M06 and B3LYP-D3BJ functional revealing similar energetics (Figure S9-S11).

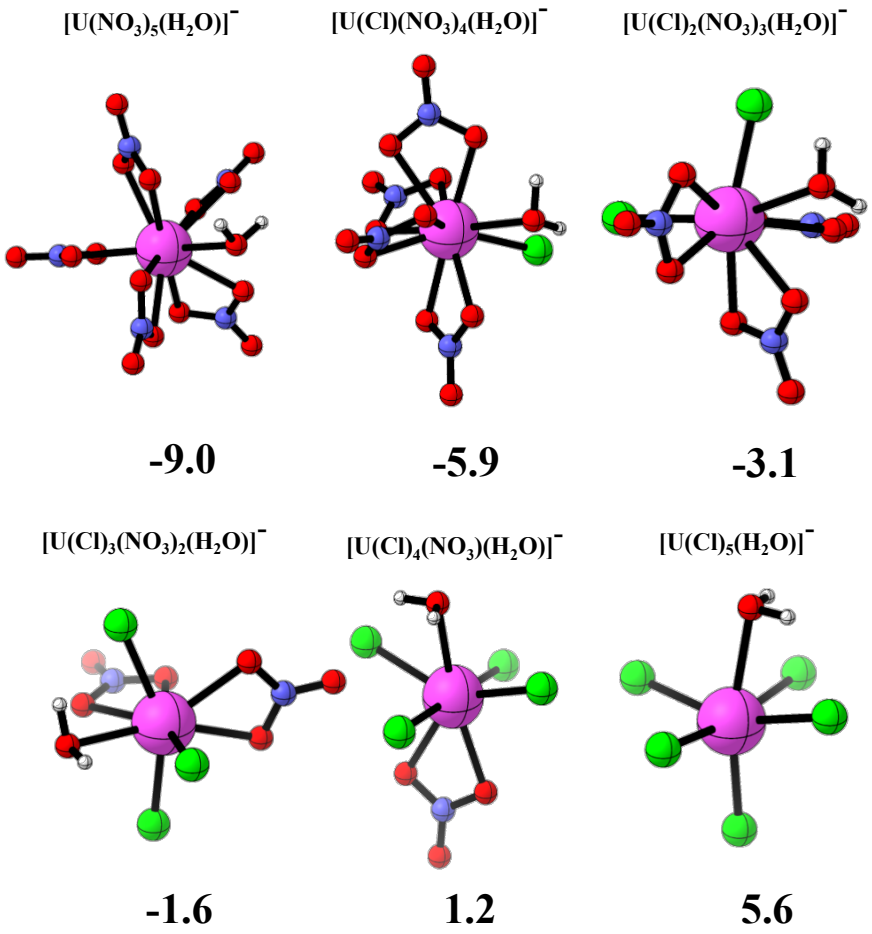

Figure 4. Low energy U(IV) mono-aqua complexes obtained from speciation of $[UCl_6]^{2-}$ at a low chloride concentration of 1 mM. The Gibbs free energy relative to $[UCl_6]^{2-}$ is reported in kcal/mol at PBE0-D3BJ/def-TZVP,def2-TZVP/COSMO//PBE0-D3BJ/def-TZVP,def2-TZVP level of theory. Color scheme: Uranium in pink, chloride in green, oxygen in red, nitrogen in blue, and hydrogen in white.

Monomeric complexes containing An-OH_2 moieties can undergo hydrolysis followed by dimerization via either oxolation or olation mechanisms. The dimerization thermodynamics of both pathways for U(IV) mono-aqua complexes (Figure 4) and the corresponding Np(IV) and Pu(IV) analogs were computed. The most stable U(IV) mono-aqua complex is $[U(NO_3)_5(H_2O)]^-$ and its dimerization after the formation of U-OH moieties via hydrolysis is discussed as a representative case (Figure 5). The Gibbs free energy for the oxolation reaction is predicted to be endergonic by +13.8 kcal/mol, which is significantly more favorable with respect to olation which is endergonic by +28.4 kcal/mol. Therefore, under thermodynamic conditions it is expected that $[U(NO_3)_5(H_2O)]^-$ would generate a U-O-U moiety (*i.e.,* the oxolation product). The dimerization Gibbs free energy for all U(IV) mono-aqua complexes, as well as for the Np(IV) and Pu(IV) analogs are presented in Table 1. The dimerization of uranium species is usually more favorable than the other studied actinides and, independently of the actinide, the oxolation dimeric products are always thermodynamically more stable than the olation ones. Therefore, An(IV) mono-aqua complexes with any Cl^-:NO_3^- ligand ratio would always prefer the formation of An-O-An moieties, the oxolation product.

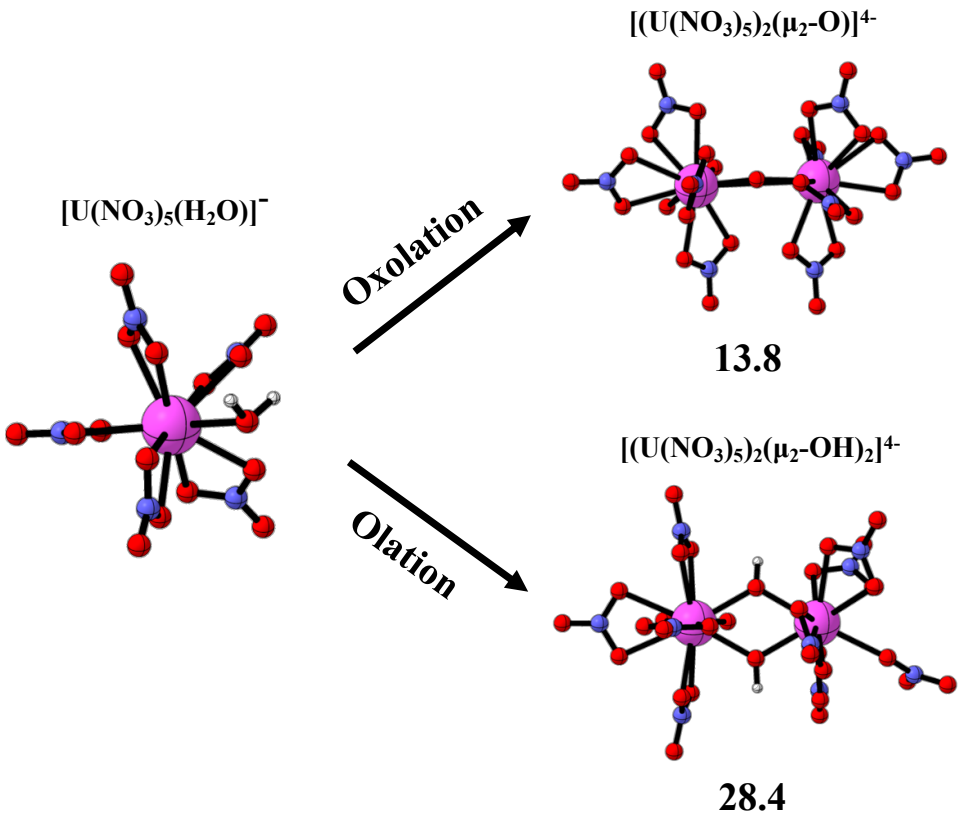

Figure 5. Gibbs free energy of the formation of the oxolation (top-right) and olation (bottom-right) dimers generated from the thermodynamically most favorable $[U(NO_3)_5(H_2O)]^-$ monomeric precursor when the chloride concentration is taken to be 1 mM. The Gibbs free energy is reported in kcal/mol at PBE0-D3BJ/def-TZVP,def2-TZVP/COSMO//PBE0-D3BJ/def-TZVP,def2-TZVP level of theory. Color scheme: Uranium in pink, oxygen in red, nitrogen in blue, and hydrogen in white.

Table 1. Gibbs free energies of formation of the oxolation and olation dimeric complexes from different monomeric actinide precursors containing one water ligand. Standard state conditions and 1M were considered for all species including water. The Gibbs free energy is reported in kcal/mol at PBE0-D3BJ/def-TZVP,def2-TZVP/COSMO//PBE0-D3BJ/def-TZVP,def2-TZVP level of theory.

	Oxolation			**Olation**		
	U	**Np**	**Pu**	**U**	**Np**	**Pu**
$[U(Cl)_5(H_2O)]^-$	-2.3	-18.6	4.6	8.3	-5.0	10.9
$[U(Cl)_4(NO_3)(H_2O)]^-$	9.6	6.2	6.0	11.6	9.4	10.8
$[U(Cl)_3(NO_3)_2(H_2O)]^-$	11.1	11.7	13.4	19.7	20.5	22.1
$[U(Cl)_2(NO_3)_3(H_2O)]^-$	8.6	13.0	13.1	18.3	20.4	22.9
$[U(Cl)(NO_3)_4(H_2O)]^-$	14.6	18.9	21.7	24.2	23.3	27.9
$[U(NO_3)_5(H_2O)]^-$	13.8	19.1	19.5	28.4	31.2	31.9

Bis-aqua complexes within 10 kcal/mol from the most stable species at the studied conditions were considered as energetically accessible for the olation and oxolation mechanisms (Figure 6). The $[U(Cl)_2(NO_3)_2(H_2O)_2]$ complex is the most stable bis-aqua complex (ΔG = 0.9 kcal/mol respect to $[UCl_6]^{2-}$), and it is presented here as a representative bis-aqua species. The formation of the hydroxo-bridged dimer (i.e., the olation product) from $[U(Cl)_2(NO_3)_2(H_2O)_2]$ is endergonic by +2.7 kcal/mol which is 5.5 kcal/mol more favorable than the formation of the oxo-bridged dimer (i.e., the oxolation product). The preference for the formation of the hydroxo-bridged dimer is also predicted in the analogous Np(IV) and Pu(IV) complexes (Table 2). Additionally, the two monomers $[An(Cl)_3(NO_3)(H_2O)_2]$ and $[An(Cl)(NO_3)_3(H_2O)_2]$ were studied (Table 3). For U(IV) bis-aqua complexes, the olation product is always thermodynamically favored over the hydroxide-bridged oxolation product. This is contrary to the mono-aqua complexes where all studied species showed a tendency towards the formation of the oxo-bridged dimer. This suggests that the formation of olation products is favored with an increase in the number of aquo ligands. The same trends are observed at M06/def-TZVP,def2-TZVP/COSMO//PBE0-D3BJ/def-TZVP,def2-TZVP level of theory. The olation and oxolation Gibbs free energies are 6.0 and 4.2 kcal/mol in average lower for actinide mono-aqua complexes, while 2.2 and 2.0 kcal/mol higher for actinide di-aqua complexes (Table S2-S3).

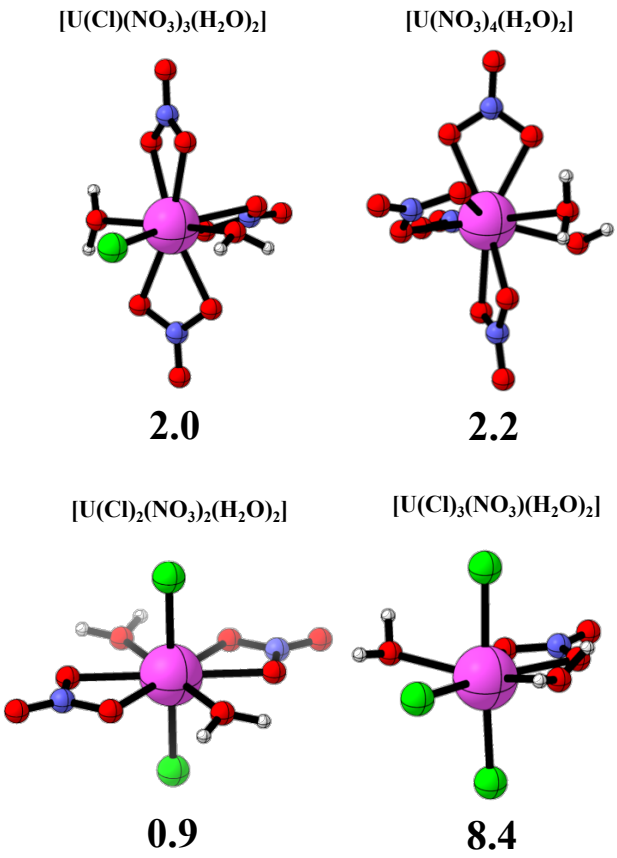

Figure 6. Low energy U(IV) bis-aqua complexes obtained from speciation of $[UCl_6]^{2-}$ at a low chloride concentration of 1mM. The Gibbs free energy relative to $[UCl_6]^{2-}$ is reported in kcal/mol at PBE0-D3BJ/def-TZVP,def2-TZVP/COSMO//PBE0-D3BJ/def-TZVP,def2-TZVP level of theory. Color scheme: Uranium in pink, chloride in green, oxygen in red, nitrogen in blue, and hydrogen in white.

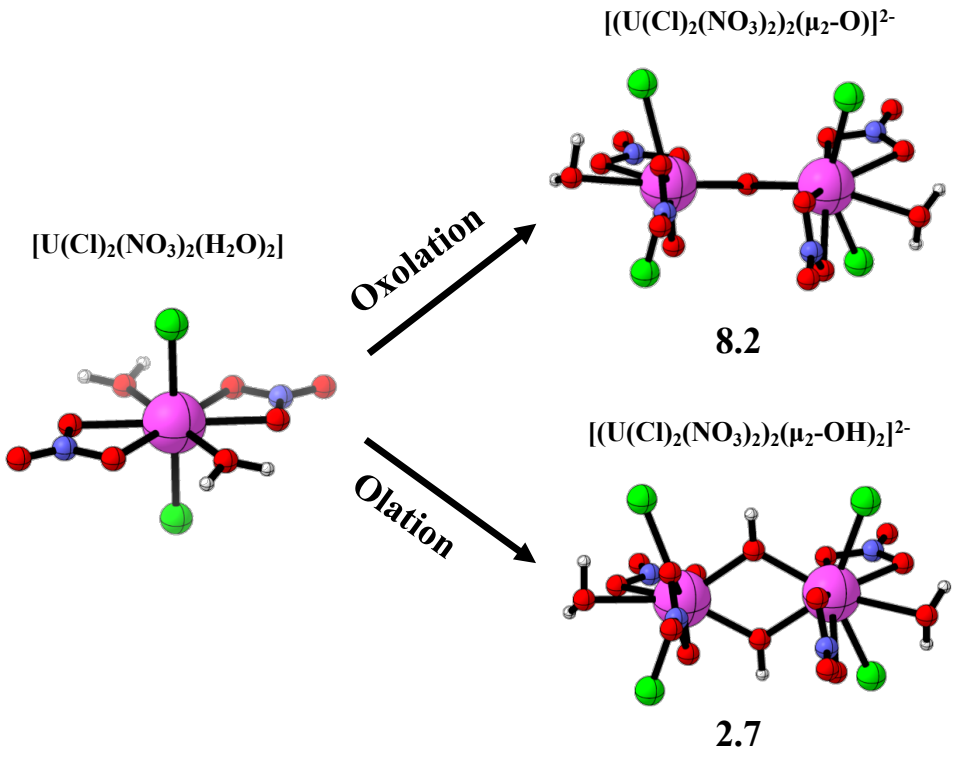

Figure 7. The Gibbs free energy of formation of the oxolation (top-right) and olation (bottom-right) dimers generated from the $[U(Cl)_2(NO_3)_2(H_2O)_2]$ bi-aqua monomeric precursor. The Gibbs free energy is reported in kcal/mol at PBE0-D3BJ/def-TZVP,def2-TZVP/COSMO//PBE0-D3BJ/def-TZVP,def2-TZVP level of theory. Color scheme: Uranium in pink, chloride in green, oxygen in red, nitrogen in blue, and hydrogen in white.

Table 2. The Gibbs free energy of formation of the oxolation and olation dimeric products from selected monomeric actinide bis-aqua precursors. Standard state conditions and 1M were considered for all species including water. The Gibbs free energy is reported in kcal/mol at PBE0-D3BJ/def-TZVP,def2-TZVP/COSMO//PBE0-D3BJ/def-TZVP,def2-TZVP level of theory.

	Oxolation			**Olation**		
	U	**Np**	**Pu**	**U**	**Np**	**Pu**
$[U(Cl)_3(NO_3)(H_2O)_2]$	-3.3	1.8	4.6	-6.1	-2.0	-1.2
$[U(Cl)_2(NO_3)_2(H_2O)_2]$	8.2	7.2	5.1	2.7	2.2	4.8
$[U(Cl)(NO_3)_3(H_2O)_2]$	19.8	-2.9	0.9	2.6	-1.2	0.6

Conclusions

The exploration of the speciation chemical space for $[An(Cl)_x(H_2O)_y(NO_3)_z]^{4-x-z}$ (An=U, Np, Pu and x=0-6, y=0-8 and z=0-6) in aqueous solution was computed in the presence of both nitrate and chloride. Ternary speciation plots were generated representative of different experimental concentrations revealing that all three $[AnCl_6]^{2-}$ species (An= U, Np, Pu) are capable of undergoing ligand exchange reactions to form actinide species with various Cl^-:NO_3^- ratios. A low concentration of chloride is required to initiate the formation of mix ligand species with a lower number of chloride ligands. All low energy mixed ligand complexes that contain at least one water have been studied as precursors for the formation of dimeric species through either oxolation or olation mechanisms. On one hand, the formation of oxo-bridged dimers through oxolation is favored when only one water is present in the complex. On the other hand, olation preferred for monomeric species that contain at two water ligands. These results are consistent with previous experimental studies; however, additional systematic speciation studies are needed to further confirm our findings. This work provides a picture of the fate of $[AnCl_6]^{2-}$ in the aqueous solution under different experimental conditions, while shedding some light on the complexity associated with the speciation of actinide species.

ASSOCIATED CONTENT

Supporting Information

The Supporting Information is available free of charge. Cartesian coordinates of all studied species, actinide speciation, olation, and oxolation energetics.

AUTHOR INFORMATION

Corresponding Author

* **Pere Miró** - Department of Chemistry, University of South Dakota, Vermillion, South Dakota 57069, United States.

ORCID ID- orcid.org/0000-0002-3281-0708; Email: pere.miro@usd.edu

Authors

Rameswar Bhattacharjee − Department of Chemistry, University of South Dakota, Vermillion, South Dakota 57069, United States.

ORCID ID- orcid.org/0000-0002-6631-5991

Author Contributions

The manuscript was written with the contributions of all authors. All authors have approved the final version of the manuscript.

ACKNOWLEDGMENT

All computations supporting this project were performed on High Performance Computing systems at the University of South Dakota funded by National Science Foundation MRI Award OAC-1626516. The authors thank the South Dakota Board of Regents for providing funding to support R. B. through the Competitive Research Grant Program. P.M. and R. B. are thankful to the Department of Chemistry at the University of South Dakota (USD) for start-up funds. The authors acknowledge that the land this research was performed on is the original homelands of the Dakota, Lakota, and Nakota tribal nations. The authors acknowledge the painful history of genocide and forced removals from this territory and honor and respect the many diverse Indigenous peoples still connected to this land on which we gather. The authors give thanks for our opportunity to gather on this land today.

REFERENCES

[1] I. Grenthe, J. Fuger, R. J. Konings, R. J. Lemire, A. B. Muller, C. Nguyen-Trung, H. Wanner, *Chemical thermodynamics of uranium, Vol. 1*, Elsevier Amsterdam, **1992**.

[2] R. Guillaumont, F. J. Mompean, *Update on the chemical thermodynamics of uranium, neptunium, plutonium, americium and technetium, Vol. 5*, Elsevier Amsterdam, **2003**.

[3] Y. Wang, M. Frutschi, E. Suvorova, V. Phrommavanh, M. Descostes, A. A. Osman, G. Geipel, R. Bernier-Latmani, *Nat. Commun.* **2013**, *4*, 1-9.

[4] S. Foti, E. Freiling, *Talanta* **1964**, *11*, 385-392.

[5] K. Bagnall, *Coord. Chem. Rev.* **1967**, *2*, 145.

[6] L. Soderholm, S. Skanthakumar, R. E. Wilson, *J. Phys. Chem. A* **2011**, *115*, 4959-4967.

[7] B. Faure, T. Kooyman, *Progress in Nuclear Energy* **2022**, *144*, 104082.

[8] Y. N. Heit, F. Gendron, J. Autschbach, *J. Phys. Chem. Lett.* **2018**, *9*, 887-894.

[9] S. G. Minasian, K. S. Boland, R. K. Feller, A. J. Gaunt, S. A. Kozimor, I. May, S. D. Reilly, B. L. Scott, D. K. Shuh, *Inorg. Chem.* **2012**, *51*, 5728.

[10] M. L. Neidig, D. L. Clark, R. L. Martin, *Coord. Chem. Rev.* **2013**, *257*, 394.

[11] D.-C. Sergentu, J. Autschbach, *Chem. Sci.* **2022**, *13*, 3194-3207.

[12] S. D. Reilly, B. L. Scott, A. J. Gaunt, *Inorg. Chem.* **2012**, *51*, 9165.

[13] S. D. Reilly, J. L. Brown, B. L. Scott, A. J. Gaunt, *Dalton Trans.* **2014**, *43*, 1498.

[14] K. E. Knope, L. Soderholm, *Chem. Rev.* **2013**, *113*, 944-994.

[15] S. Abeysinghe, D. K. Unruh, T. Z. Forbes, *Cryst. Growth Des.* **2012**, *12*, 2044.

[16] M. B. Andrews, C. L. Cahill, *Chem. Rev.* **2013**, *113*, 1121.

[17] D. D. Schnaars, R. E. Wilson, *Inorg. Chem.* **2013**, *52*, 14138.

[18] E. Bossé, C. Den Auwer, C. Berthon, P. Guilbaud, M. S. Grigoriev, S. Nikitenko, C. L. Naour, C. Cannes, P. Moisy, *Inorg. Chem.* **2008**, *47*, 5746.

[19] S. I. Nikitenko, C. Hennig, M. S. Grigoriev, C. L. Naour, C. Cannes, D. Trubert, E. Bossé, C. Berthon, P. Moisy, *Polyhedron* **2007**, *26*, 3136.

[20] S. Siegel, *Acta Crystallogr.* **1956**, *9*, 827.

[21] J. Su, P. D. Dau, H. T. Liu, D. L. Huang, F. Wei, W. Schwarz, J. Li, L. S. Wang, *J. Chem. Phys.* **2015**, *142*, 134308.

[22] R. E. Wilson, *Inorg. Chem.* **2015**, *54*, 10208.

[23] R. E. Wilson, D. D. Schnaars, M. B. Andrews, C. L. Cahill, *Inorg. Chem.* **2014**, *53*, 383.

[24] J. N. Wacker, M. Vasiliu, K. Huang, R. E. Baumbach, J. A. Bertke, D. A. Dixon, K. E. Knope, *Inorg. Chem.* **2017**, *56*, 9772-9780.

[25] J. N. Wacker, S. Y. Han, A. V. Murray, N. A. Vanagas, J. A. Bertke, J. M. Sperling, R. G. Surbella, K. E. Knope, *Inorg. Chem.* **2019**, *58*, 10578-10591.

[26] W. von der Ohe, *J. Chem. Phys.* **1975**, *63*, 2949.

[27] S. G. Minasian, J. M. Keith, E. R. Batista, K. S. Boland, D. L. Clark, S. D. Conradson, S. A. Kozimor, R. L. Martin, D. E. Schwarz, D. K. Shuh, G. L. Wagner, M. P. Wilkerson, L. E. Wolfsberg, P. Yang, *J. Am. Chem. Soc.* **2012**, *134*, 5586.

[28] S. G. Balasubramani, G. P. Chen, S. Coriani, M. Diedenhofen, M. S. Frank, Y. J. Franzke, F. Furche, R. Grotjahn, M. E. Harding, C. Hattig, A. Hellweg, B. Helmich-Paris, C. Holzer, U. Huniar, M. Kaupp, A. Marefat Khah, S. Karbalaei Khani, T. Muller, F. Mack, B. D. Nguyen, S. M. Parker, E. Perlt, D. Rappoport, K. Reiter, S. Roy, M. Ruckert, G. Schmitz, M. Sierka, E. Tapavicza, D. P. Tew, C. van Wullen, V. K. Voora, F. Weigend, A. Wodynski, J. M. Yu, *J. Chem. Phys.* **2020**, *152*, 184107.

[29] J. P. Perdew, K. Burke, M. Ernzerhof, *Phys. Rev. Lett.* **1996**, *77*, 3865.

[30] S. Grimme, J. Antony, S. Ehrlich, H. Krieg, *J. Chem. Phys.* **2010**, *132*, 154104.

[31] M. Ernzerhof, G. E. Scuseria, *J Chem. Phys.* **1999**, *110*, 5029-5036.

[32] S. Grimme, S. Ehrlich, L. Goerigk, *J. Comput. Chem.* **2011**, *32*, 1456.

[33] F. Weigend, *Phys. Chem. Chem. Phys.* **2002**, *4*, 4285.

[34] F. Weigend, R. Ahlrichs, *Phys. Chem. Chem. Phys.* **2005**, *7*, 3297.

[35] F. Weigend, *Phys. Chem. Chem. Phys.* **2006**, *8*, 1057.

[36] A. Klamt, G. Schüürmann, *J. Chem. Soc., Perkin Trans. 2* **1993**, 799.

[37] A. Schäfer, A. Klamt, D. Sattel, J. C. Lohrenz, F. Eckert, *Phys. Chem. Chem. Phys.* **2000**, *2*, 2187.

[38] T. Sata, T. Yamaguchi, K. Matsusaki, *J. Phys. Chem.* **1995**, *99*, 12875-12882.

[39] A. Montes-Rojas, J. Rentería, N. Chávez, J. Ávila-Rodríguez, B. Y. Soto, *RSC adv.* **2017**, *7*, 25208-25219.

[40] V. Weber, D. Asthagiri, *J. Chem. Phys.* **2010**, *133*, 141101.

[41] C. P. Kelly, C. J. Cramer, D. G. Truhlar, *J. Phys.Chem. B* **2006**, *110*, 16066-16081.

[42] E. Rossini, E. W. Knapp, *J. Comp. Chem.* **2016**, *37*, 1082-1091.

[43] J. R. Pliego Jr, J. M. Riveros, *Phys. Chem. Chem. Phys.* **2002**, *4*, 1622-1627.

[44] V. S. Bryantsev, M. S. Diallo, W. A. Goddard Iii, *J. Phys. Chem. B* **2008**, *112*, 9709-9719.

[45] Y. Zhao, D. G. Truhlar, *Theor. Chem. Acc.* **2008**, *120*, 215-241.

[46] Y. Zhao, D. G. Truhlar, *J. Chem. Phys.* **2006**, *125*, 194101.

[47] A. D. Becke, *J. Chem. Phys.* **1993**, *98*, 5648.

[48] A. D. Becke, *Phys. Rev A* **1988**, *38*, 3098.

[49] C. Lee, W. Yang, R. G. Parr, *Phys. Rev. B: Condens. Matter Mater. Phys.* **1988**, *37*, 785.

[50] C. Y. Legault, *Université de Sherbrooke (http://www.cylview.org)* **2020**.

[51] M. Henry, J. P. Jolivet, J. Livage, in *Chemistry, Spectroscopy and Applications of Sol-Gel Glasses*, Springer, **1992**, pp. 153-206.

[52] L. Chatelain, R. Faizova, F. Fadaei-Tirani, J. Pécaut, M. Mazzanti, *Angewandte Chemie International Edition* **2019**, *58*, 3021-3026.

[53] N. P. Martin, C. Volkringer, N. Henry, X. Trivelli, G. Stoclet, A. Ikeda-Ohno, T. Loiseau, *Chemical science* **2018**, *9*, 5021-5032.

[54] B. Biswas, V. Mougel, J. Pécaut, M. Mazzanti, *Angewandte Chemie International Edition* **2011**, *50*, 5745-5748.

[55] N. P. Martin, C. Volkringer, P. Roussel, J. März, C. Hennig, T. Loiseau, A. Ikeda-Ohno, *Chemical Communications* **2018**, *54*, 10060-10063.

[56] J. K. Gibson, R. G. Haire, *Journal of alloys and compounds* **2001**, *322*, 143-152.

[57] G. Nocton, F. Burdet, J. Pecaut, M. Mazzanti, *Angewandte Chemie* **2007**, *119*, 7718-7722.

[58] J. Diwu, J. J. Good, V. H. DiStefano, T. E. Albrecht-Schmitt, Wiley Online Library, **2011**.

[59] K. E. Knope, L. Soderholm, *Inorganic Chemistry* **2013**, *52*, 6770-6772.

[60] C. Tamain, T. Dumas, D. Guillaumont, C. Hennig, P. Guilbaud, *European Journal of Inorganic Chemistry* **2016**, *2016*, 3536-3540.

[61] J. Diwu, S. Wang, T. E. Albrecht-Schmitt, *Inorganic Chemistry* **2012**, *51*, 4088-4093.

[62] K. Takao, S. Takao, A. C. Scheinost, G. Bernhard, C. Hennig, *Inorganic Chemistry* **2012**, *51*, 1336-1344.

[63] I. Colliard, C. Falaise, M. Nyman, *Inorg. Chem.* **2020**, *59*, 17049-17057.

[64] D. Ray, J. Xie, J. White, G. E. Sigmon, L. Gagliardi, A. E. Hixon, *Chem. Eur. J.* **2020**, *26*, 8115-8120.

[65] K. E. Knope, S. Skanthakumar, L. Soderholm, *Inorg. Chem.* **2015**, *54*, 10192-10196.

Table of Contents